

Supporting Information for:

Charge transport in graphene-polythiophene blends as studied by Kelvin Probe Force Microscopy and transistor testing

Andrea Liscio,^a Giulio Paolo Veronese,^b Emanuele Treossi,^a Francesco Suriano,^b Francesco Rossella,^c Vittorio Bellani,^c Rita Rizzoli,^{b*} Paolo Samori^{d,*} and Vincenzo Palermo^{a*}

^a ISOF – Consiglio Nazionale delle Ricerche, via Gobetti 101, 40129 Bologna, Italy. Fax: +39 051 6399844; Tel: +39 051 6399844; E-mail: palermo@isof.cnr.it

^b IMM – Consiglio Nazionale delle Ricerche, via Gobetti 101, 40129 Bologna, Italy. Fax: +39 051 6399216; Tel: +39 051 6399131; E-mail: rizzoli@bo.imm.cnr.it

^c Dipartimento di Fisica "A. Volta" and CNISM, Università di Pavia, via Bassi 6, 27100 Pavia – Italy

^d Nanochemistry Laboratory, ISIS – CNRS 7006, Université de Strasbourg, 8 allée Gaspard Monge, 67000 Strasbourg, France. Fax: +33 (0)368 855236; Tel: +33 (0)368 855160; E-mail: samori@unistra.fr

SAMPLE PREPARATION AND UNIFORMITY

Samples with reduced graphene oxide (RGO) on native and thick SiO_x are realised by i) spin coating graphene oxide (GO) sheets in water solution and after ii) annealing them at 700°C at P= 3x10⁻⁶ mbar.

Four GO concentrations are used: 0.25, 0.5, 1 and 2 g L⁻¹ corresponding to a percentage coverage that varies linearly (fig. 5). The solution of GO was spin coated at 2000 rpm.

Should be noted that, thanks to the high processability of the GO, not only the sheet density but also the average sheet size could be controlled using different sonication times to have GO sheets suitable for different kind of measurements: we used sheets of tens of microns for visualization by fluorescence quenching microscopy (fig 4 c,d) and Raman microscopy, sheets of micron size for the KPFM measurements (fig. 1 - 4a,b – S5); sheets of hundreds of nm range for FET preparation (fig. 4e).

Chemical exfoliation does not yield monodispersed sheets; in particular, in FET preparation we used a sheet size much smaller than the channel length, i.e. the scalelength on which charge is transported. The same GO batch, having the same sheet size distribution, has been used for all the FET described in the paper, to have a fair comparison.

P3HT from BASF Chemicals (MW < 50,000, regioregularity > 98 %) was dissolved in anhydrous chloroform, heated at 70 °C for 10 min. cooled at room temperature, filtered through a 0.45 µm pore size PTFE membrane syringe filter and spin coated at 1400 rpm on the substrates. To remove the solvent the samples were heated at 100°C for 30 min under argon atmosphere.

The thickness of P3HT was ~5 nm for AFM and Kelvin measurements and ~30 nm for FET devices.

In fig. S1 are reported the SEM images of the samples obtained using different GO concentrations (the samples are indicated with A1-A4 for the four concentrations) showing in the insets AFM images acquired on the same samples. Fig. S2 displays SEM images at different magnifications for concentrations of (a) 0.25 g L^{-1} and (b) 1 g L^{-1} as an example, enhancing the high uniformity of the GO deposition over the substrate even on the hundreds of micron scale. It is important to note that the thermal annealing process does not modify the morphology of the surfaces. Thus, the coverage values achieved for GO agree with those obtained with RGO. In general, SEM and AFM images allow to acquire two complementary information: SEM images allow to perform a large statistic over areas of few mm^2 , while AFM images can detect the presence of single and multi-layers.

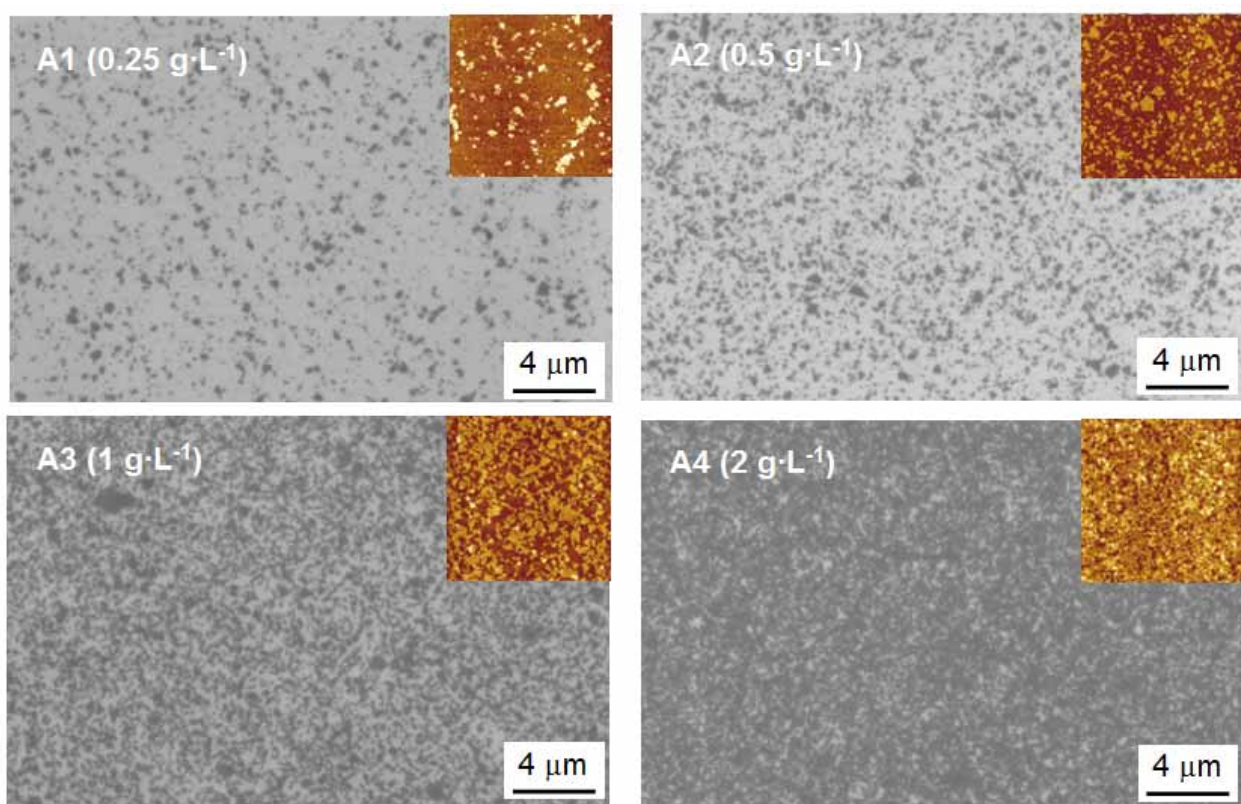


Fig. S1 SEM images of graphene sheets obtained at different concentrations: (A1) = 0.25 g L^{-1} , (A2) = 0.5 g L^{-1} , (A3) = 1 g L^{-1} , and (A4) = 2 g L^{-1} . In the insets, an AFM image of each sample reported with the same data scale. Z range of inserts = 3 nm.

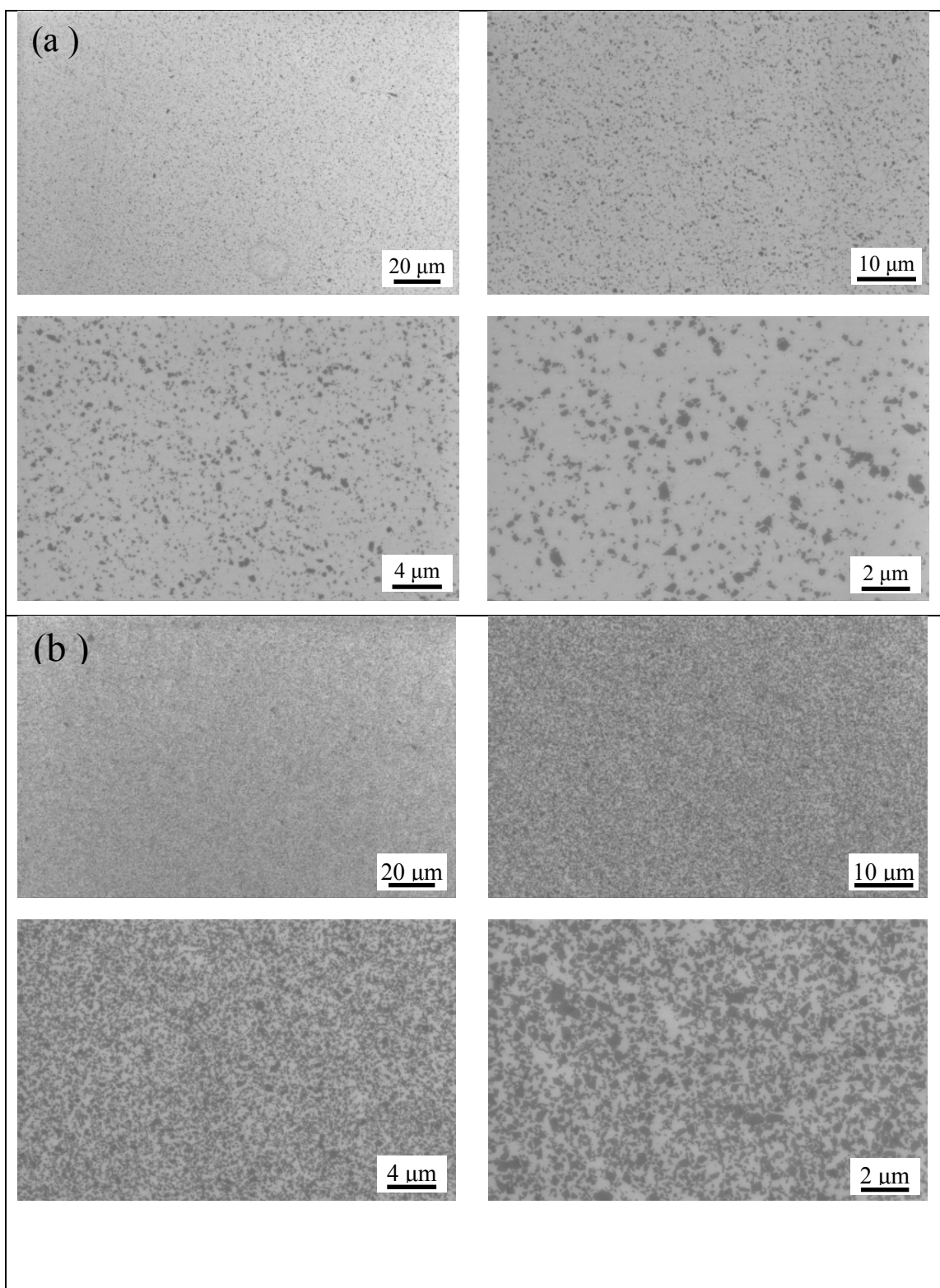


Fig. S2 SEM images of graphene sheets obtained at different magnifications. (a) $0.25 \text{ g}\cdot\text{L}^{-1}$ and (b) $1 \text{ g}\cdot\text{L}^{-1}$ concentrations.

RAMAN COMPARISON OF “SCOTCH TAPE” GRAPHENE, GO AND RGO

To better understand the fine structure of the graphene layer, we performed Raman spectra of the GO and RGO, together with the spectrum of “conventional” exfoliated graphene (Fig. S3). The latter exhibits a sharp G-peak, while GO and RGO show wide D- and G-bands¹. We find that the G-band of both GO and RGO is shifted to higher frequencies with respect to the G-peak of exfoliated graphene, and this G-peak shift is usually related to doping by chemisorption or physisorption of molecules, ions, functional groups or metal particles², that can take place in the fabrication process of the GO. Moreover, we find that the overall Raman peak intensities are decreased after the thermal treatment, suggesting a partial loss of carbon during reduction³ (in Fig. S3 the spectrum of RGO has been multiplied by a factor ~ 2 in order to equal the G-peak intensity of the spectrum of GO). After reduction we observe a small increase of the intensity ratio $I(D)/I(G)$ (from 1.30 to 1.35), finding a similar trend the area ratio $A(D)/A(G)$. In fact during reduction GO undergoes structural changes due to the loss and rearrangement of oxygen and carbon atoms, which affect the Raman response. Given that the reported measurements were performed on large sheets of GO and RGO, with lateral dimensions larger than the laser spot, the appearance of the prominent D-band with intensity comparable with that of the G-band, along with the large width of these bands, are indicative of an important structural disorder^{1,4}. These observations show that GO and RGO feature a very similar degree of disorder; the reduction process, thus, does not re-establish the pristine graphenic lattice, but has the only function of restoring conjugation of the carbon bonds which survived to the initial oxidation process.

Raman scattering measurements were carried out with a micro-Raman spectrometer (Horiba Jobin-Yvon), using a $100\times$ objective (laser spot diameter $\sim 1\text{ }\mu\text{m}$), with a spectral resolution of $\sim 1\text{ cm}^{-1}$, laser excitation wavelength of 632.8 nm and power $\sim 4\text{ mW}$.

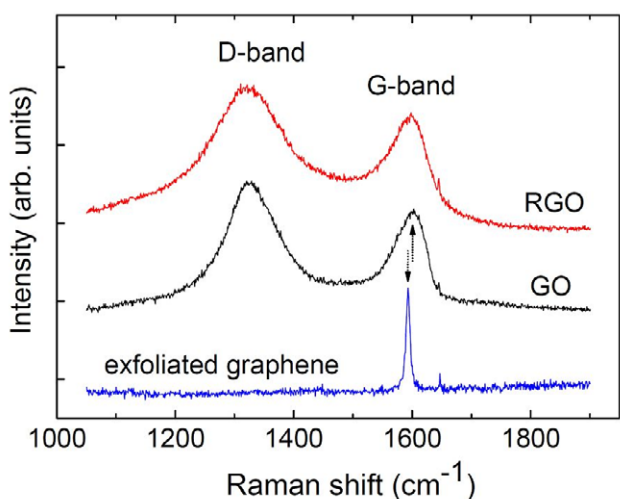


Fig. S3. The Raman spectra of GO, RGO and exfoliated graphene in the region of D- and G-band. The spectra were normalized to the G-band intensity. The arrows visualize the shift of the G-band.

IMAGE PROCESSING

Bare substrate and GO (RGO) sheets have been unambiguously distinguished in all the topographic images, as shown in fig. S4a, where the sheets are identified by darker regions with polygonal shape while the surrounding light areas correspond to the bare substrate. This false-colour scale is converted into numerical values using an image processing software. In the fig. S4b is displayed an example of the image analysis used, performed in this case on a profile taken by tracing a line (red dash line) in the SEM image. A pore analysis is performed by applying a threshold filter (blue dash-dot line) to the data recorded on SEM images. All the pixels individuated by the regions marked in blue in fig. S4b correspond to the GO (or RGO) sheets.

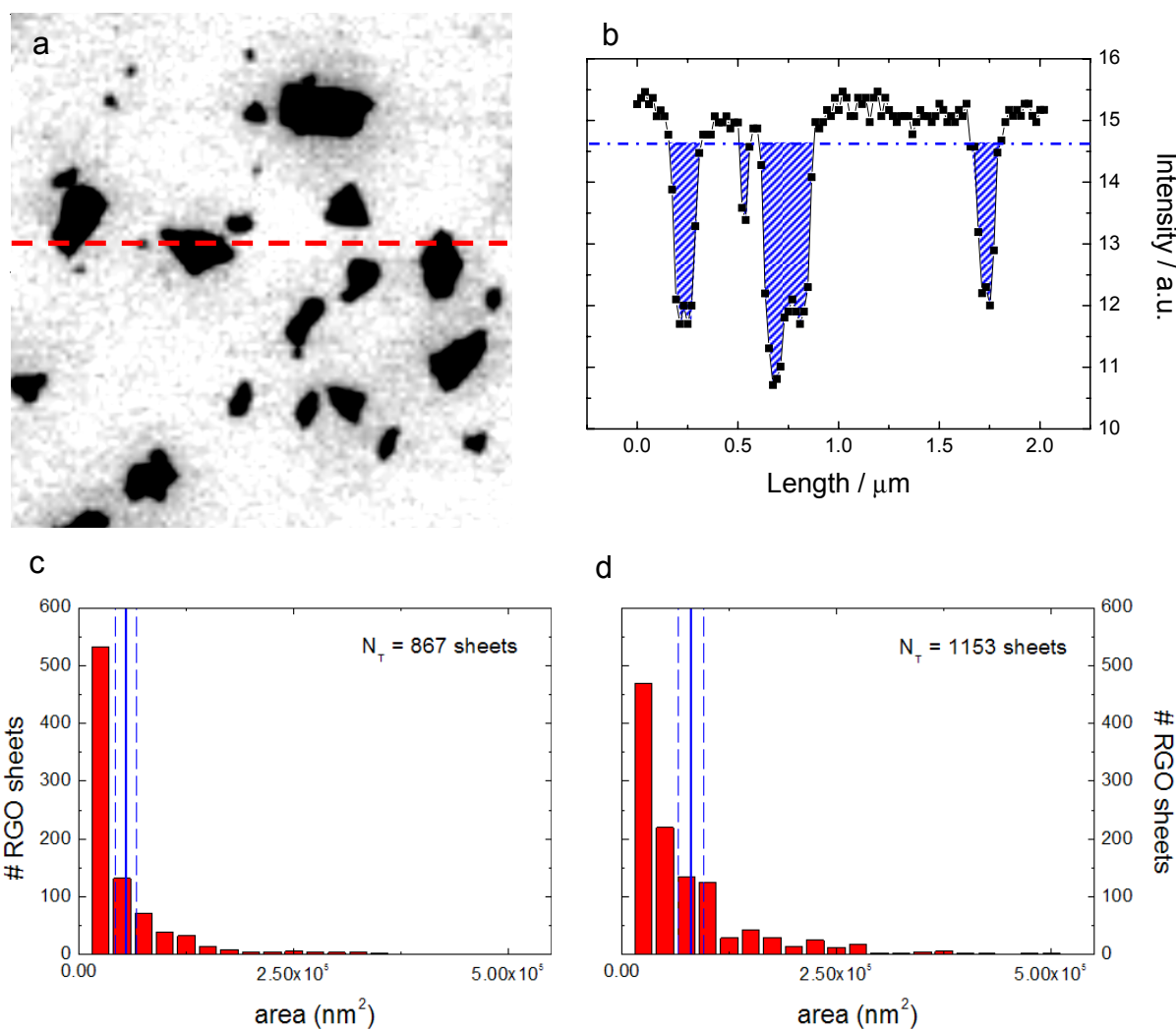


Fig. S4 a) A SEM image and b) the profile corresponding to the red line traced in the 2D image by tracing a line. The threshold value is marked as a blue dash dotted line which identifies the sheets (blue regions) from the substrate. Frequency counts of the observed GO sheets for c) $0.25 \text{ g}\cdot\text{L}^{-1}$ and d) $= 0.5 \text{ g}\cdot\text{L}^{-1}$. Mean values and corresponding error bars are represented with vertical blue lines.

Fig. S4b represents a 1D analysis for the sake of simplicity. In general, SEM and AFM images are converted to a M×L matrix where the sheets are defined as “negative islands” left when the image landscape is flooded to the threshold level (i.e. image segmentation algorithm). Hence, the sheet coverage is defined as:

$$\text{coverage} = \frac{N_{\text{sub-thr}}}{M \times L} \times 100\% \quad (\text{S1})$$

where $N_{\text{sub-thr}}$ corresponds to the number of the pixels having the intensity value smaller than the threshold.

The analysis of the sheet sizes is performed collecting all the SEM images. The frequency count (f) obtained with the segmentation algorithm is reported in Fig. S4 for two concentrations: c) $0.25 \text{ g}\cdot\text{L}^{-1}$ and d) $= 0.5 \text{ g}\cdot\text{L}^{-1}$, using a step sampling of $2.5 \cdot 10^4 \text{ nm}^2$.

About one thousand of sheets are observed for both batches of samples over a total scanned area of $420 \mu\text{m}^2$. Both f distributions are peaked at $2.5 \cdot 10^4 \text{ nm}^2$ even if the tail increases with the concentration.

The mean area value (\bar{A}) and the corresponding variance (σ_A^2) are calculated as weighted average:

$$\bar{A} = \sum_{i=1}^R \tilde{f} \cdot A_i, \quad \sigma_A^2 = \frac{1}{R-1} \sum_{i=1}^R \tilde{f} \cdot (\bar{A} - A_i)^2, \quad \tilde{f} = f / N_{\text{tot}} \quad (\text{S2})$$

Where A_i is the area of i^{th} -sheet, R and Ntot represent the total number of steps used to collect the data in the frequency count and the total number of observed sheets, respectively.

The calculated mean area values amounting to $(55 \pm 13) \cdot 10^3 \mu\text{m}^2$ and $(80 \pm 14) \cdot 10^3$, for $0.25 \text{ g}\cdot\text{L}^{-1}$ and $0.5 \text{ g}\cdot\text{L}^{-1}$ concentrations, are shown in Fig. S2c,d (blue vertical lines).

The SEM analysis is used to obtain statistical data on the area coverage, and then complemented with AFM analysis which allows to discriminate single layers from bi- or multi-layers. Apart from the highest concentration, though, the samples can be assumed to be covered by mostly monolayers on the whole surface, as confirmed by AFM.

AFM AND KPFM COMPARISON OF GO AND RGO SHEETS

GO and RGO sheets show different electrical properties (i.e. insulator and conductive sheets) which can be studied with KPFM measurements. AFM images of (a) GO and (b) RGO spun on native SiO_x are shown in Fig. S5 (conc = 0.5 g·L⁻¹) while the corresponding KPFM images are shown in Fig. S5c,d. We note that the measured WF on GO does not vary between the first and the second layer (marked with circle). Differently, in the case of RGO a WF dependence with the number of layer is achieved and reported in Fig. 3 in the main text. In the Fig. S5d these differences are directly visualised in the KPFM image where it is clear to distinguish the different WF of (0) substrate, (1) first and (2) second RGO layer, while the WF of the third layer is less evident.

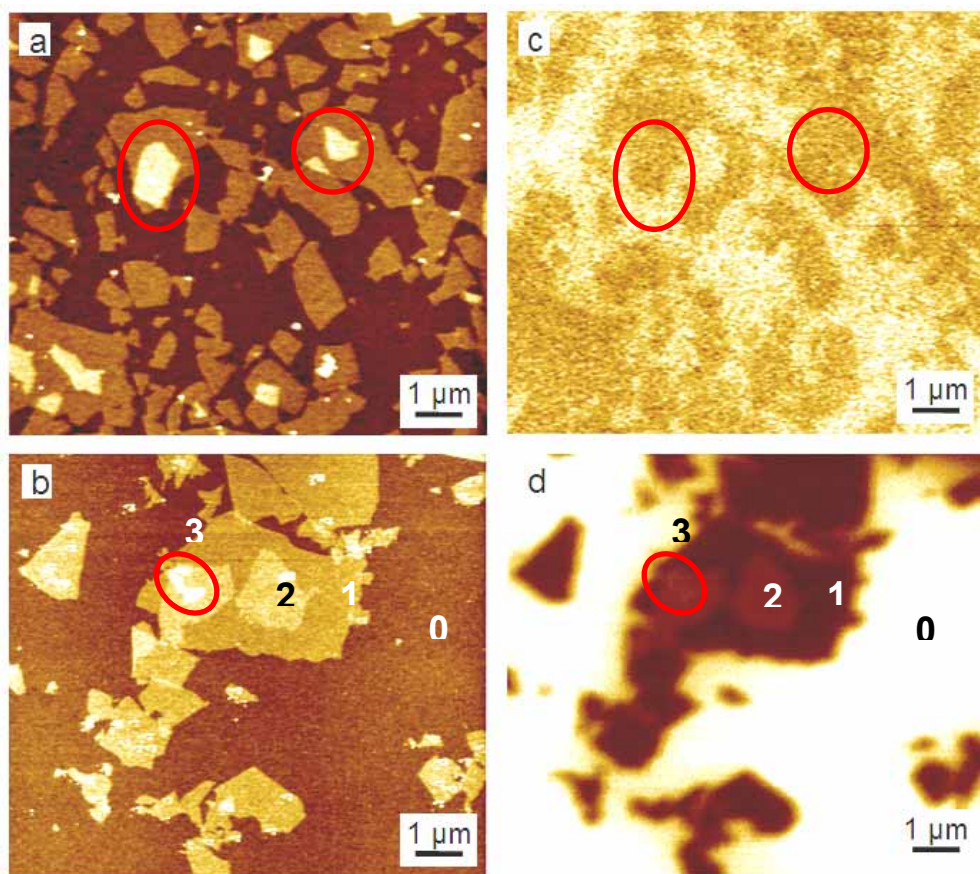


Fig. S5 AFM images of (a) GO and (b) RGO sheets on native SiO_x and corresponding (c,d) KPFM images. Z ranges: (a) = 4 nm, (b) = 6 nm, (c) = 150 mV and (d) 250 mV.

TRANSISTOR ARCHITECTURES

Silicon substrates (n-type, resistivity 0.01-0.02 Ohm·cm) have been used for the fabrication of the transistors. A 225 nm thick silicon dioxide (SiO_2) has been thermally grown after standard RCA1&2 cleaning processes of the native wafers. Interdigitated transistor devices have been fabricated defining source-drain electrodes by means of standard lift-off processes (Fig. S6). Channel lengths of 10 and 60 μm have been used, with a constant width-to-length ratio of 200. Both bare silicon oxide substrates and RGO sheets covered substrate have been utilized for the FETs fabrication. Electrodes have been realized by e-beam evaporation of 25 nm thick Ni layer. Silicon substrates have been used as bottom gate electrode. The P3HT thin film, ~30 nm thick, has been then spin coated on the substrates.

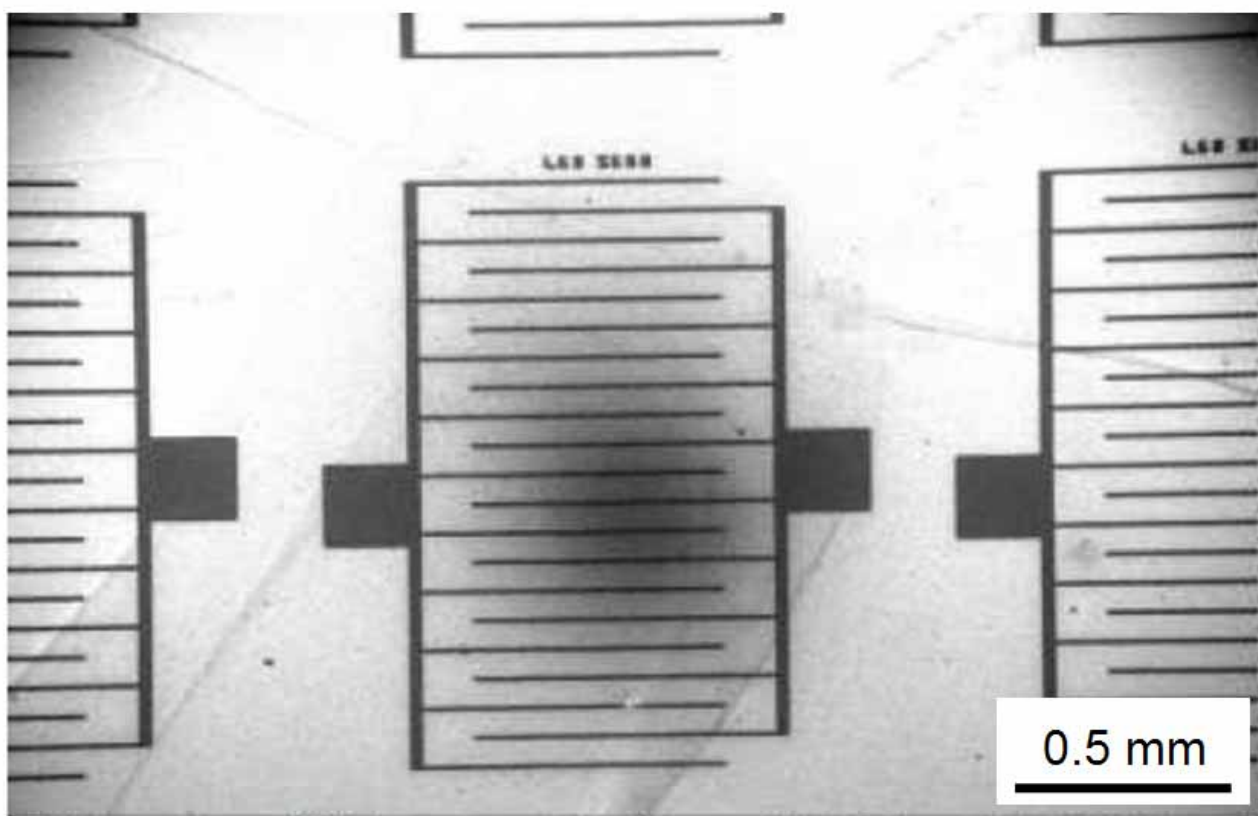


Fig. S6 SEM image of the transistor architecture used for FET measurements (W/L = 200, channel length of 60 μm)

REFERENCES

1. M. A. Pimenta, G. Dresselhaus, M. S. Dresselhaus, L. G. Cancado, A. Jorio and R. Saito, *Physical Chemistry Chemical Physics*, 2007, **9**, 1276-1291.

2. G. Eda and M. Chhowalla, *Adv. Mat.*, **22**, 2392-2415.
3. Z. Q. Wei, D. E. Barlow and P. E. Sheehan, *Nano Letters*, 2008, **8**, 3141-3145.
4. M. Chhowalla, A. C. Ferrari, J. Robertson and G. A. J. Amaralunga, *Appl. Phys. Lett.*, 2000, **76**, 1419-1421.